SUPPORTING MATERIALS

The effect of DNA CpG methylation on the dynamic conformation of a nucleosome

Isabel Jimenez-Useche[1], Chongli Yuan[1*]

1. **Supporting methods**
2. **Supporting figures**
3. **Supporting references**

1. SUPPORTING METHODS

1.1 Fluorescence labeling efficiency

The TAMRA labeling efficiency of a DNA fragment can be calculated as the ratio of TAMRA dye and DNA concentrations using equations S1 and S2 (1).

$$[Dye] = A_{558} / \varepsilon_{TAMRA,558} \qquad \text{(S1)}$$

$$[DNA] = \frac{A_{260} - [Dye]\varepsilon_{TAMRA,260}}{\varepsilon_{DNA,260}} \qquad \text{(S2)}$$

in which,

$A_{wavelength}$: the absorption of a labeled sample at a given wavelength;

$\varepsilon_{TAMRA,wavelength}$: the extinction coefficient of TAMRA at a given wavelength, i.e., $\varepsilon_{TAMRA,558}$ = 91000 $M^{-1}cm^{-1}$ and $\varepsilon_{TAMRA,260}$ = 29100 $M^{-1}cm^{-1}$ (2);

$\varepsilon_{DNA,260}$: the extinction coefficient of a double-stranded DNA

The TAMRA labeling efficiency is determined using DNA samples with only TAMRA labels. The TAMRA labeling efficiency of unmethylated and methylated DNA is calculated to be both larger than 99%.

1.2 Analysis approach of time-domain fluorescence decay curves

For each measurement, we obtain a fluorescence decay curve which is then analyzed to reveal the number of distinctive fluorescence species (n) and their respective fluorescence lifetimes (τ_i). The number of fluorescence species (n) is determined using the following approach. For each decay curve, we start with a one-species model. If the model correctly captures the data trend, the fitting results will yield a χ^2 value close to 1.0 and residuals randomly distributed around zero. A poor fitting model, on the other hand, will result in χ^2 >>1 and a distinguishable pattern in the residuals plot (Fig. S3 and Fig. 4). If it occurs, we will increase n by 1, i.e., using a two-species model. These steps will be repeated iteratively. By judging the quality of our fitting results, we will determine n as the **minimum** number of fluorescence species essential to fit the fluorescence decay curve. For example, if two fluorescence species coexist in the sample, increasing n from 2 to 3 will not improve the fitting quality and we will take n as 2. The aforementioned analysis approach is commonly used to determine n of a typical fluorescence decay curve. The lifetime of each distinctive fluorescence species can be obtained using Eq.1 by fixing n.

To verify the feasibility of utilizing time-domain fluorescence spectroscopy to distinguish multiple fluorescence species, we prepared an equimolar mixture of two distinctive fluorescence species with known lifetime and collected its corresponding fluorescence decay curve. These two species were fluorescently labeled DNA fragments (A and B) with a lifetime of τ_A = 3.59 ± 0.01 ns and τ_B = 2.67 ± 0.01 ns as measured independently. The decay curve of the mixture was analyzed as described before. The one component fitting model gave a single lifetime (τ) of 3.17 ±0.01 ns (with a χ^2 of 1.53 and non-randomly distributed residuals). The two component fitting gave two lifetimes, τ_1 and τ_2, of 3.74 ± 0.06 ns and 2.56 ± 0.06 ns, and a fraction of species A as 0.54 ± 0.04 (with a χ^2 of 0.97 and randomly distributed residuals around zero). This experiment

verified the feasibility of using time-domain fluorescence decay curves to resolve distinctive fluorescence species that coexist in a sample.

The fluorescence decay curves of our nucleosomes labeled with FAM and TAMRA at the DNA ends are consistently best fitted using a two-component model, which indicates the existence of two distinctive fluorescence species. The fitting parameters, i.e. two lifetimes τ_1 and τ_2 and the corresponding fractions f_1 and f_2 are used to calculate the DNA end-to-end distance in nucleosomes and the corresponding equilibrium constants between the two nucleosome conformations. The lifetimes and the fractions are coupled with each other in the fitting model. The experimental error bars reported in our data are standard deviations of multiple experimental readouts. The error bars reported in this study are typical to a time-domain fluorescence experiment. We perform multiple batches of DNA preparation, nucleosome reconstitutions and fluorescence measurements to increase our sample size and verify the statistical significance of our findings. For the results presented in Fig.5-Fig.7, we conduct statistical analysis (unpaired *t*-test with equal variances) to examine the significance of our measured datasets. The *p*-values are reported in the figure captions.

1.3 Anisotropy measurements

Time-domain anisotropy decay curves of FAM labeled nucleosomes were collected using a ChronosBH lifetime spectrophotometer (ISS, Champaign, IL). The steady state anisotropy of TAMRA or FAM labeled nucleosomes was measured using a SpectraMax M5 Microplate Reader (Molecular Devices, Sunnyvale, CA). The experiments were performed under various salt type and different salt concentrations and the results are summarized in Figs.S5-S10.

The anisotropy values of both FAM and TAMRA dye exhibit no dependence on the type or the concentration of salt. The measured anisotropy values are consistently lower than 0.25. The estimated distance using energy transfer efficiency is therefore expected to have <10% error (3).

1.4 Förster distance (R_0) calibration

We monitor the Förster distance (R_0) of the specific dye pair, i.e., FAM-TAMRA, using a short DNA fragment. Specifically, we utilize PAGE purified 17bp dsDNA fragments (CGGACTCCAGGTCACCC) with appropriate fluorescence labels. This short DNA fragment behaves as a rigid rod with a fixed end-to-end distance, c.a., 60Å (calculated as 17bp×3.4Å/bp + 2.5Å due to dye labeling (5)) under different ionic strengths. The energy transfer efficiency is calculated using the fluorescence lifetime of the FAM-only and the dual-labeled DNA samples. The values of R_0 under various salt concentrations can be calibrated and are shown in Fig.S4. The calculated Förster distance exhibits no dependence on the salt concentration.
The R_0 value was also calculated using the spectral properties of the donor and the acceptor molecules using the equation S3 (6):

$$R_0^6 = \frac{9000\,(\ln 10)\kappa^2 Q_D}{128\pi^5 N n^4} J(\lambda) \qquad \text{(S3)}$$

The R_0 value was found to be 51.9Å. These result is in close agreement with our experimental calculation of R_0 (50.3Å) using a 17bp dsDNA fragment as a molecular ruler.

2. SUPPORTING FIGURES

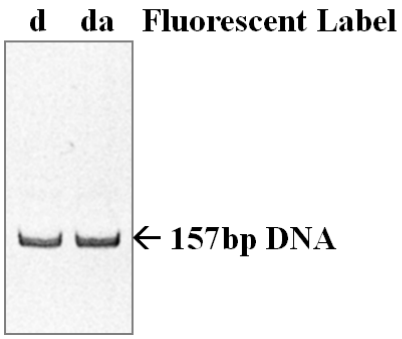

Figure S1. A typical 10% PAGE showing the quality of the fluorescently labeled 157bp DNA fragments. *d* and *da* indicate FAM-labeled and dual-labeled DNA fragments respectively. The gel was run using 0.5xTBE buffer at room temperature, 150V and visualized using ethidium bromide.

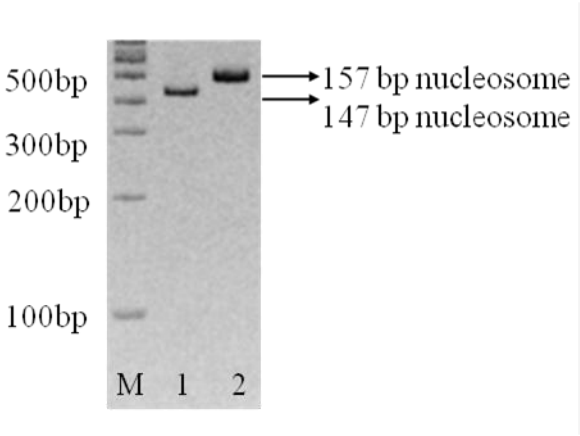

Figure S2. A typical 8% polyacrylamide gel of reconstituted nucleosome samples. M: 100 bp NEB DNA ladder. Lane 1: nucleosomes reconstituted with 147bp DNA and Lane 2: nucleosomes reconstituted with 157bp DNA. Both nucleosomes in lanes 1 and 2 were reconstituted *in vitro* using recombinant *Xenopus laevis* histones. The gel was run using 0.25xTBE buffer, at 4^{o}C, 150V and stained with ethidium bromide.

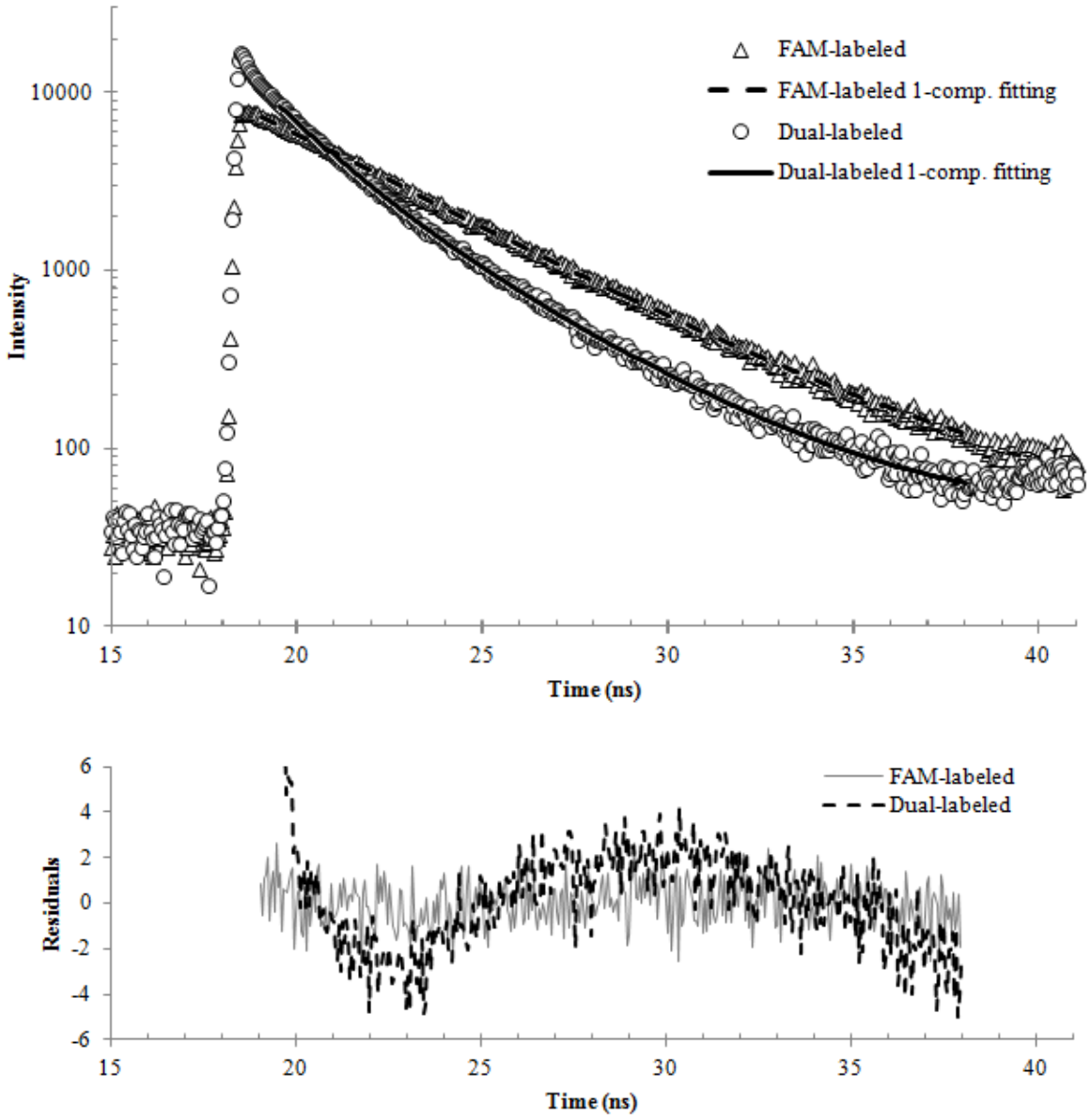

Figure S3: Typical time-domain fluorescence decay curves of FAM-labeled (χ^2=1.0, τ=4.06ns) and dual-labeled (χ^2=4.82, τ=2.63ns) nucleosomes, fitted using a one-component model.

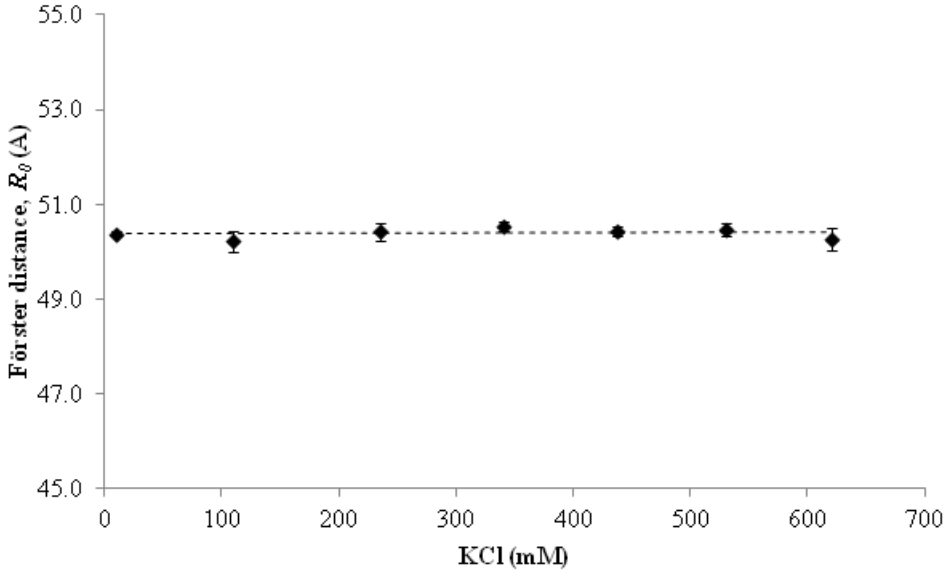

Figure S4. The effect of KCl concentrations on the Förster distance of a FAM-TAMRA FRET pair. R_0 remains at a constant value of 50.3 ± 1.7Å.

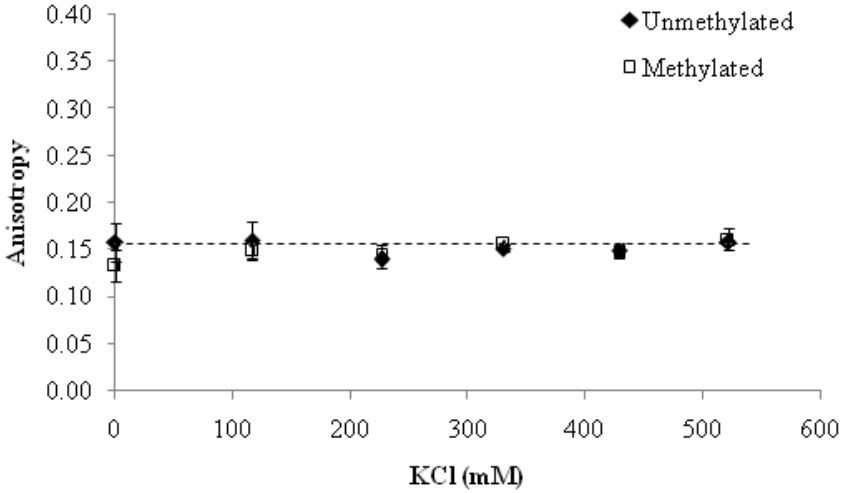

Figure S5. The effect of monovalent counterions on the anisotropy of FAM-labeled nucleosomes.

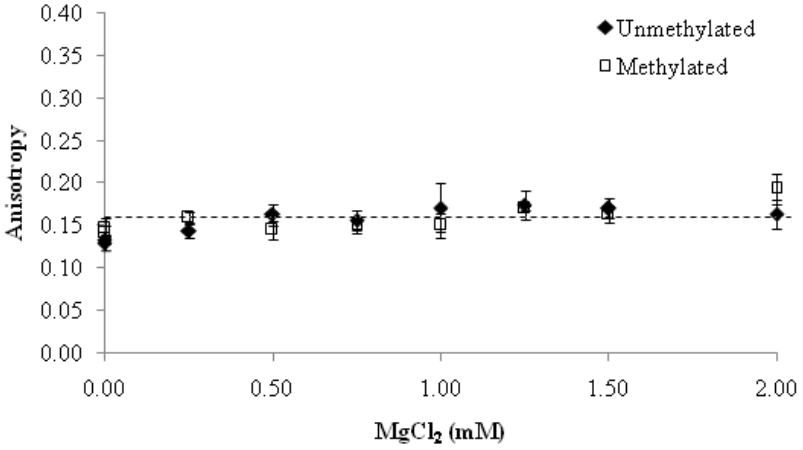

Figure S6. The effect of divalent counterions on the anisotropy of FAM-labeled nucleosomes.

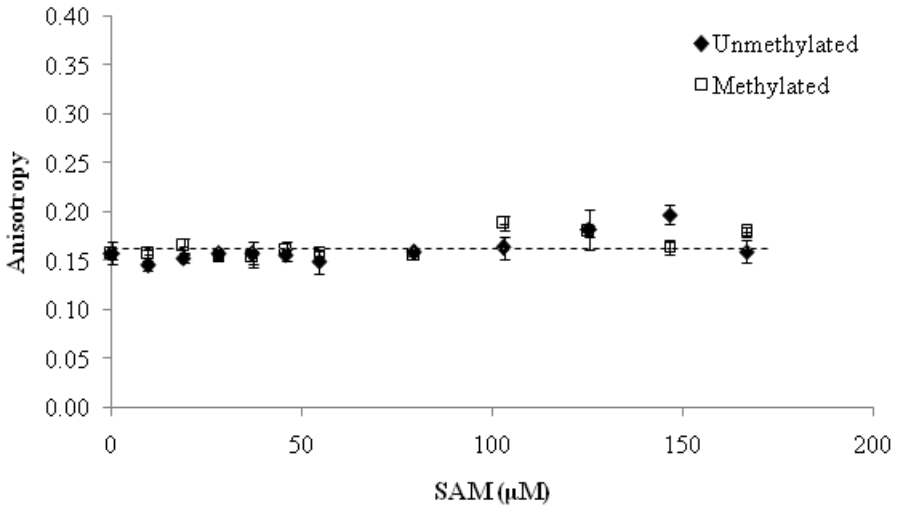

Figure S7. The effect of S-adenosylmethionine (SAM) on the anisotropy of FAM-labeled nucleosomes.

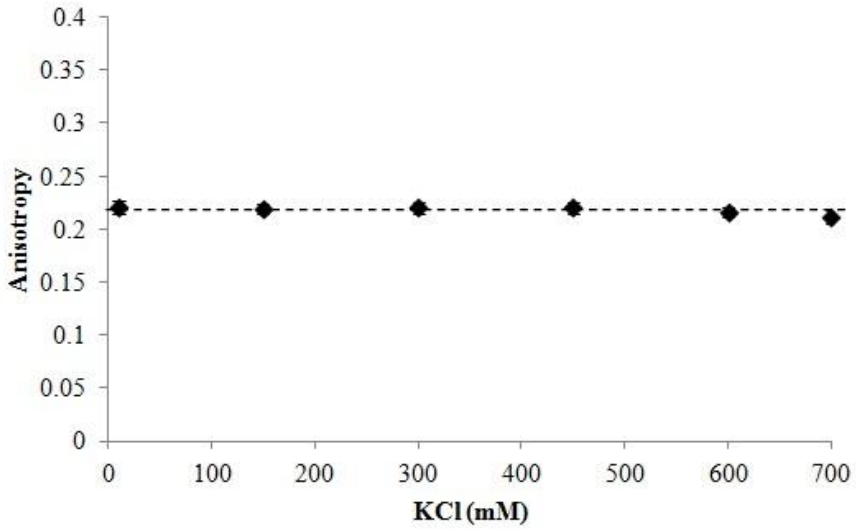

Figure S8. The effect of monovalent counterions on the anisotropy of unmethylated TAMRA-labeled nucleosomes.

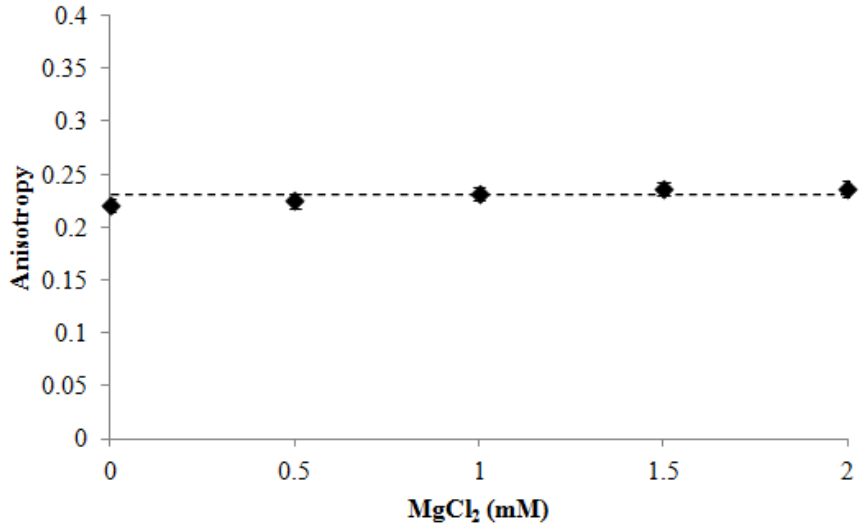

Figure S9. The effect of divalent counterions on the anisotropy of unmethylated TAMRA-labeled nucleosomes

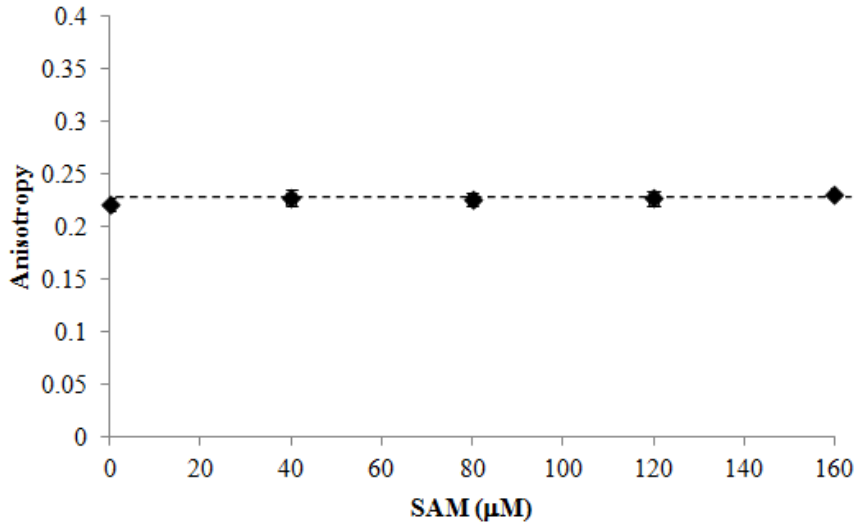

Figure S10. The effect of S-adenosylmethionine (SAM) on the anisotropy of unmethylated TAMRA-labeled nucleosomes.

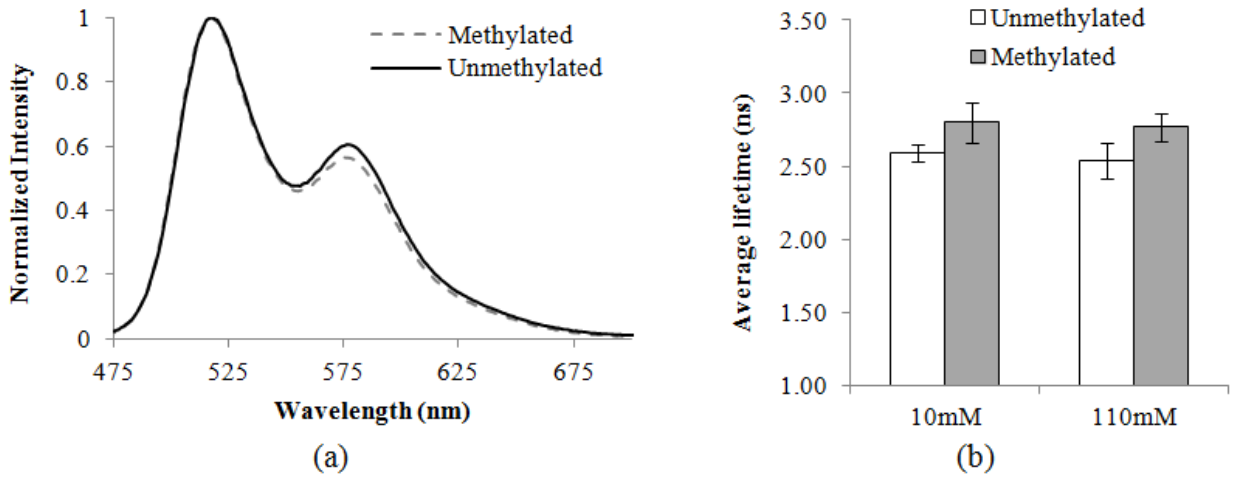

Figure S11. Steady-state and time-resolved fluorescence lifetime measurements of nucleosomes reconstituted with a 157bp DNA fragment containing Widom-601 sequence. The TAMRA and the FAM labels are located on the DNA end and the octamer surface. The serine 47 of a histone H4 was mutated to a cystein for the site-specific labeling of a FAM dye to a histone octamer. (a) The emission spectra of the dual-labeled methylated and unmethylated nucleosome samples are collected using a Cary Eclipse fluorophotometer with an excitation wavelength of 440nm. The spectra are normalized to the maximum emission at 520nm. The intensity of the TAMRA emission peak at 570nm is therefore proportional to the energy transfer efficiency. DNA methylation leads to lower energy transfer efficiency that suggests a less compact nucleosome structure. (b) The averaged fluorescence lifetimes of dual-labeled nucleosomes at 10mM and 110mM KCl. Methylated nucleosomes exhibit higher fluorescence lifetimes that correspond to lower energy transfer efficiencies and less compact nucleosome conformations.

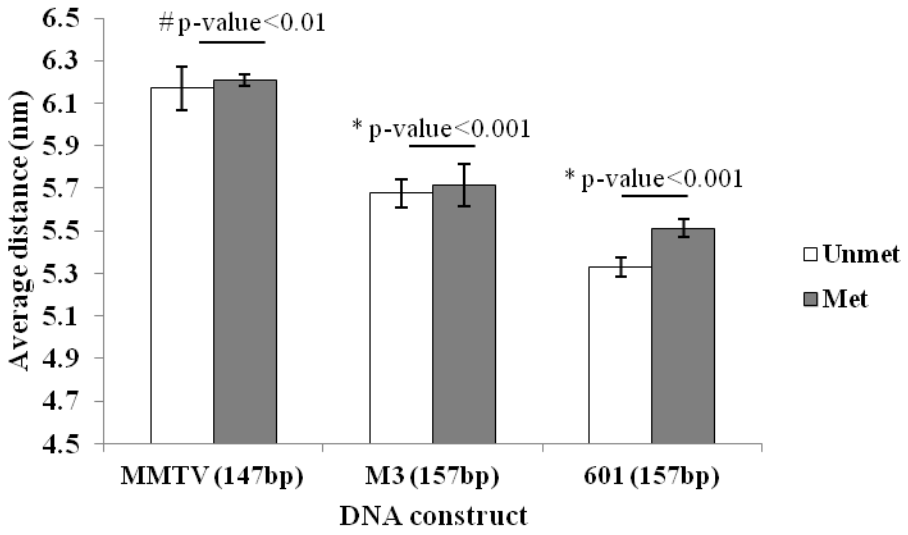

Figure S12. Average DNA end-to-end distances of nucleosomes with different DNA constructs measured at 100mM KCl. The FRET labels are located at the DNA ends. The average distance is calculated as $f_1 d_1 + (1-f_1) d_2$, where d_1 and d_2 are the distances in the compact and open conformations respectively, and f_1 is the fraction of nucleosomes in the compact conformation. MMTV is a 147bp DNA containing 10 CpG sites, with the following sequence: ACTTGCAACA GTCCTAACAT TCACCTCTTG TGTGTTTGTG TCTGTT**CG**CC ATCC**CG**TCTC **CG**CT**CG**TCAC TTATCCTTCA CTTTCCAGAG GGTCCCCC**CG** CACACCC**CG**G **CG**ACCCTCAG GT**CG**GC**CG**AC TG**CG**GCACAG TTTTTTG. M3 is a 157bp DNA containing 19 CpG sites with the following sequence: *ATCCC*CTGGA GAATCC**CG**GT GC**CG**AGGC**CG** CTCAATTGGT **CG**TAGACAGC TCTAGCAC**CG** CTTAAA**CG**CA **CG**TA**CGCG**CT GTCCCC**CGCG** TTTT**CG**C**CG**C CAAG**CG**GATT ACTC**CG**TAGT CTCC**CG**GCA**C G**TGT**CG**GATA TATACATCCT GT*GCGAT*. The average end-to-end distance of the Widom-601 (157bp), as reported in the manuscript, is included here for comparison. Nucleosomes with higher methylation level exhibit a less compact conformation in all cases.

3. SUPPORTING REFERENCES

1. Edelman, L.M., Cheong, R., Kahn, J.D. (2003) Fluorescence Resonance Energy Transfer over ~130 Basepairs in Hyperstable Lac Repressor-DNA Loops. Biophysical Journal, ***84***, 1131–1145.
2. You, Y., Tataurov, A.V., Owczarzy, R. (2011) Measuring Thermodynamic Details of DNA Hybridization Using Fluorescence. Biopolymers, ***95***, 472-486.
3. Haas, E., Katchalskikatzir, E. & Steinberg, I.Z. (1978). Effect of orientation of donor and acceptor on probability of energy-transfer involving electronic-transitions of mixed polarization. *Biochemistry* **17**, 5064-5070.
4. Sambrook, J. and Russell, D.W. (2001) Isolation of DNA Fragments from Polyacrylamide Gels by the Crush and Soak Method in Molecular Cloning. 3rd edition. Cold Spring Harbor Laboratory Press. Cold Spring Harbor, NY.
5. Stuhmeier, F., Welch, J. B., Murchie, A.I. H. , Lilley, D.M. J., Clegg, R.M. (1997) Global Structure of Three-Way DNA Junctions with and without Additional Unpaired Bases: A Fluorescence Resonance Energy Transfer Analysis. Biochemistry, ***36***, 13530-13538
6. Stryer, L. (1976) Fluorescence Energy Transfer as A Spectroscopic Ruler, *Ann. Rev. Biochem.*, ***47***, 819-846.